Virology 408 (2010) 197–203

Contents lists available at ScienceDirect

Virology

journal homepage: www.elsevier.com/locate/yviro

DNA condensates organized by the capsid protein VP15 in White Spot Syndrome Virus

Yingjie Liu [a,c,1], Jinlu Wu [b,1], Hu Chen [c], Choy Leong Hew [b,c,*], Jie Yan [a,c,d,*]

[a] Department of Physics, National University of Singapore, 2 Science Drive 3, Singapore 117542, Singapore
[b] Department of Biological Science, National University of Singapore, 14 Science Drive 4, Singapore 117543, Singapore
[c] Mechanobiology Institute, 5A Engineering Drive 1, Singapore 117411, Singapore
[d] Centre for Bioimaging Sciences, National University of Singapore, 14 Science Drive 4, Singapore 117543, Singapore

ARTICLE INFO

Article history:
Received 23 June 2010
Returned to author for revision
23 July 2010
Accepted 9 September 2010
Available online 16 October 2010

Keywords:
WSSV
VP15
DNA condensation
Magnetic tweezers
AFM

ABSTRACT

The White Spot Syndrome Virus (WSSV) has a large circular double-stranded DNA genome of around 300 kb and it replicates in the nucleus of the host cells. The machinery of how the viral DNA is packaged has been remained unclear. VP15, a highly basic protein, is one of the major capsid proteins found in the virus. Previously, it was shown to be a DNA binding protein and was hypothesized to participate in the viral DNA packaging process. Using Atomic Force Microscopy imaging, we show that the viral DNA is associated with a (or more) capsid proteins. The organized viral DNA qualitatively resembles the conformations of VP15 induced DNA condensates *in vitro*. Furthermore, single-DNA manipulation experiments revealed that VP15 is able to condense single DNA against forces of a few pico Newtons. Our results suggest that VP15 may aid in the viral DNA packaging process by directly condensing DNA.

Introduction

Chromosomal DNA in most of eukaryotic cells is compacted into nucleosome-based chromatin. However in some eukaryotes, prokaryotes, and viruses, DNA compaction is not based on the formation of nucleosomes. For example, in bacteria, the compaction is contributed mostly by DNA bending or bridging proteins (Dame, 2005). In DNA viruses, the compaction is achieved mostly by interaction between DNA and capsid proteins (Borca et al., 1996; Krishnamoorthy et al., 2003; Luijsterburg et al., 2008; Sun et al., 2008). Compared to the understanding of how DNA is packaged in eukaryotes and bacteria, DNA packaging by capsid proteins in viruses is much less studied.

Discovered in South Asia at the beginning of the 1990s, the White Spot Syndrome Virus (WSSV) has brought a devastating epidemic to shrimp industry. It belongs to the virus family Nimaviridae, genus *Whispovirus* (Mayo, 2002) and has a circular double-stranded DNA (dsDNA) genome of around 300 kb. The ovoidal WSSV particles have a dimension about 275 nm in length and 120 nm in width, with a tail-like appendage at one end. Its nucleocapsid is rod-shaped surrounded by a trilaminar envelope. Isolated nucleocapsids have a crosshatched appearance and a size of about 300×70 nm (Durand et al., 1998). The WSSV shares many characteristics with non-occluded baculoviruses including its virion particle shape, nuclear localization, and its ultrastructure (shape, size, orientation) (Bud and Kelly, 1980; Durand et al., 1998).

Generally, the viral genome packaging mechanism is poorly understood for viruses that contain dsDNA genomes and replicate in the host cell nucleus. It is highly energetically costly to compact the large genomes of these viruses into their tiny capsids. The complete DNA packaging machinery is not known. However, it is believed that some folding proteins may aid in the packaging process. Some viruses directly utilize host histones for DNA packaging (for examples, polyomaviruses and papillomaviruses). Some viruses encode their own DNA packaging proteins (for examples, adenovirus and herpesviruses) (Hunt, 2010).

Since WSSV shares many characteristics with baculoviruses, we pay special attention to how DNA is packed in baculoviruses. No histones have been found in baculovirus virions. Instead, there is evidence that the baculovirus genome DNA is associated with a small (15 kDa), very basic protein in virions (Bud and Kelly, 1980; Tweeten et al., 1980; Wilson et al., 1987). This protein has been believed to aid in the condensation of the large viral genome DNA during the packaging process (Wilson and Miller, 1986). In addition to this DNA condensation protein, motor proteins that utilize ATP may also be involved to package the DNA. A candidate of the motor protein, ac66, was identified in the baculovirus (Braunagel et al., 2003; Deng et al., 2007). However, an ac66

* Corresponding authors. J. Yan is to be contacted at the Department of Physics, National University of Singapore, 2 Science drive 3, Singapore 117542, Singapore. Fax: +65 6777-6126. C.L. Hew, at the Department of Biological Science, National University of Singapore, 14 Science Drive 4, Singapore 117543, Singapore.
E-mail addresses: phyyj@nus.edu.sg (Y. Liu), dbshewcl@nus.edu.sg (C.L. Hew).
[1] These authors contributed equally to the research.

0042-6822/$ – see front matter © 2010 Elsevier Inc. All rights reserved.
doi:10.1016/j.virol.2010.09.008

knockout virus, although not viable, was found still able to package the DNA into the capsid (Ke et al., 2008). It was also reported that actin of the host cell might be involved in the viral DNA packaging process (Lanier and Volkman, 1998).

Much research has focused on the structural proteins of WSSV and nine major nucleocapsid structural proteins have been identified (Li et al., 2007; van Hulten et al., 2002). Among them, VP15 is a highly basic protein located in the nucleocapsid with a theoretical molecular mass of 6.7 kDa and a pI of 13.2 (Witteveldt et al., 2005). In SDS-PAGE gel, VP15 displays a band corresponding to a molecular mass of 15 kDa (van Hulten et al., 2002). Earlier studies suggesting VP15 binding to DNA were based on electrophoretic mobility shift assay (EMSA) (Witteveldt et al., 2005; Zhang et al., 2001). More recent studies showed that VP15 can interact with itself to form homomultimers, but not with the other major structural proteins of WSSV (Witteveldt et al., 2005). The above points suggest that VP15 may play a similar role to the 15 kDa highly basic protein associated with the DNA in baculovirus virions.

Details of how VP15 interacts with DNA remain unclear. This research aims to investigate the mechanism using single-molecule imaging and manipulation methods. The VP15 mediated DNA condensates were imaged using an Atomic Force Microscopy (AFM), and were compared with the viral DNA leaked from fractured WSSV capsids. The strength of the VP15 induced DNA condensation was investigated by studying single-DNA condensation against controlled forces using a transverse magnetic tweezer setup described previously (Yan et al., 2004). We expect the knowledge obtained in our study will be useful in further elucidating the possible roles of VP15 in the viral genome packaging process.

Results and discussion

Direct visualization of WSSV genome DNA organization

As mentioned in the Introduction, there were evidences that the baculovirus genome DNA is associated with a small (15 kDa), very basic protein in virions (Bud and Kelly, 1980; Tweeten et al., 1980; Wilson et al., 1987). In order to know whether the WSSV genome DNA is organized similarly, we imaged WSSV virion particles and particularly focused on those which had ruptured during the purification and sample preparation for AFM imaging. Fig. 1A shows

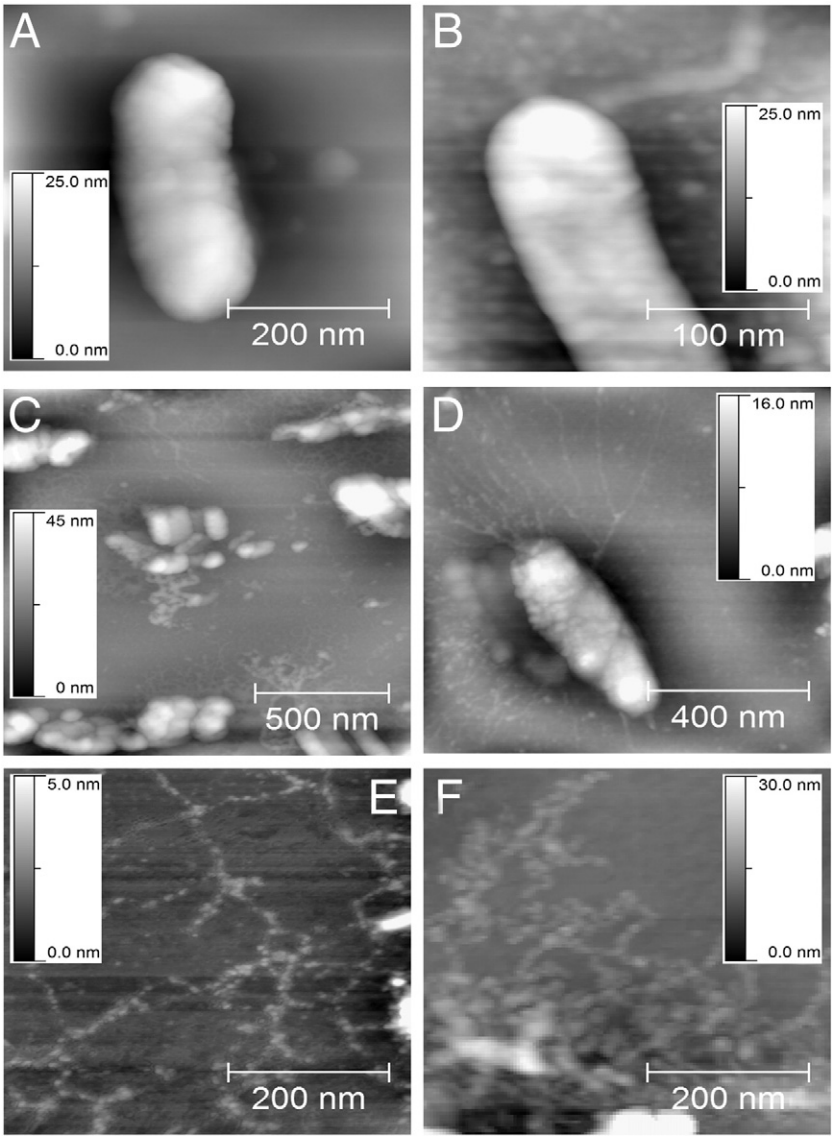

Fig. 1. AFM images of WSSV viral particles and genome DNA leaked from fractured virions. (A–B) Two virion particles without and with a tail-like appendage, respectively. (C–D) Degraded and fractured virions. Filament bundles or networks, presumably the leaked viral genome DNA, often surrounded the degraded or fractured virions. (E–F) Images of the filament structures surrounding the degraded or fractured virions show bundles and complex networks. Nucleosome-like particles were often seen on these filament structures. These characteristic images were chosen from around 50 micrographs we analyzed.

a virion, which is an ovoidal particle of about 335 nm in length and 135 nm in diameter. Its tail-like appendage was lost during the sample preparation. Fig. 1B shows another virion which still kept its tail-like appendage. These observations were in agreement with previously reported WSSV virion and nucleocapsid structures (Durand et al., 1998).

During sample preparation, some virions were degraded or fractured (Figs. 1C–D). Complex network structures composed of thin filaments were often seen around the fracture virions. In contrast with the observation, such structures were never seen around intact virions (Figs. 1A–B). The large genome DNA (around 300 kb) is the most likely candidate that could form such thin filament based large complex network structures. We presume that these structures are the WSSV genome DNA condensed by one or a few capsid proteins. Most often, the type of DNA condensates seen is a network of bundles (Figs. 1E–F). In addition, nucleosome-like particle structures were often observed on the DNA condensates (Figs. 1E–F). It is known that the baculovirus genome DNA is associated with a single small (15 kDa), highly basic protein in the virions. Since WSSV and the baculoviruses share many characteristics (Bud and Kelly, 1980; Durand et al., 1998), and since VP15 is a small, highly basic nucleocapsid protein found in WSSV, it is reasonable to propose that VP15 is most likely to be one of the major protein components bound to the WSSV genome DNA condensates. To see how this is possible, we imaged DNA condensates induced by VP15 alone.

AFM imaging revealed various structures of folded DNA

Fig. 2 shows AFM images of Phix174 DNA-VP15 complexes at different VP15 concentrations. Figs. 2A–B show two characteristics often seen in structures of DNA condensates in 66 nM of VP15: (1) bridging of remote DNA sites forming large DNA loops (Fig. 2A) and (2) synergizing many DNA together forming a flower-like structure with a protein-rich center and protein-free DNA surrounding the center (Fig. 2B). At this concentration, a large portion of DNA backbone was unbound by VP15. When the concentration of VP15 was increased to 660 nM, the DNA was condensed into tightly folded, networked DNA bundles (Figs. 2C–D). No unbound DNA was observed at this concentration. At VP15 concentrations of 6.6 nM or less, DNA are mostly unbound by VP15 (Supplementary Fig. S1).

Comparing with the ~300 kb WSSV genome DNA, the 5386 bp Phix174 DNA used in the images in Fig. 2 is much shorter. It would be interesting to see whether the DNA size and sequence might affect the structures of the DNA condensates. Therefore, we also imaged VP15 mediated DNA condensates for 48,502 bp λ-DNA molecules. In addition to be much longer than Phix 174, λ-DNA has very different sequence composition from Phix 174. At 660 nM VP15, Figs. 2E–F show that the λ-DNA were also tightly folded into bundles that resemble those observed for Phix174 DNA (Figs. 2C–D) imaged at the same concentration. When VP15 concentration was increased to 6.6 μM, striking nucleosome-like structures formed on the condensed λ-DNA (Figs. 2G–H). These particles resemble the structures observed from DNA that was leaked from fractured virions (Figs. 1C–F). Overall, the main similarities between WSSV genome DNA and VP15 induced DNA condensates are cross linked bundles at low VP15 concentrations and particle-like structures at high VP15 concentrations.

VP15 can fold DNA against tensile forces

Fig. 3A shows an experiment at a concentration of 6.6 nM of VP15. VP15 resulted dynamical changes of the DNA extension were observed apparently at 1.24 pN, 0.55 pN, and 0.22 pN. DNA compaction was not observed at concentrations less than 6.6 nM in the force range (>0.2 pN). Therefore, we concluded that 6.6 nM is close to a minimal concentration that was required for DNA packaging by VP15.

Figs. 3B–C show DNA compaction at 33 nM and 66 nM, respectively. Complex folding behavior was observed. An increase in the concentration by two times resulted in a dramatic increase in the overall folding rate by more than 10 times at the higher force. Under these concentrations, the folding time courses did not show regular stepwise signals, suggesting that folding was not caused by the formation of simple regular local structures. For each condition at 6.6 nM, 33 nM, and 66 nM, we conducted between 3 to 8 experiments. Although the folding time courses varied, the general behavior is the same. At 6.6 nM, we never observed large scale folding in the force range >0.1 pN (we did not reduce force to below 0.1 pN). At 33nM, large scale folding always occurred instantly when the force was dropped to around 3 pN. Similarly, large scale folding always occurred instantly when the force was dropped to 5 pN in 66 nM VP15. We emphasize that these numbers do not have any equilibrium thermal dynamics meaning. It is absolutely possible that folding could occur at larger than 5 pN forces if the DNA was held for longer time. Our intention was to demonstrate that VP15 could quickly fold DNA against forces of a few pN. It was observed that using the same amount of force, increasing the VP15 concentration increases the speed of the folding. On the contrary, when using the same concentration, applying a larger force lowers the folding speed.

Figs. 4A–B show the unfolding dynamics under large forces. The DNA folded in 6.6 nM VP15 solution could be nearly fully unfolded under ~3 pN (Fig. 4A). The unfolding was stepwise, which was in agreement with the intermittent stepwise folding time course observed in Fig. 3A (see the time course at 0.59 pN). Such signals can be explained if the folding was caused by synergizing remote DNA sites together, by which DNA loops formed. Under large forces, the synergies were broken, leading to the sudden increase in extension. The DNA folded in 33 nM VP15 required much larger force for unfolding. Fig. 4B shows that even a force of 13 pN could not completely unfold the DNA in 20 min. In addition, unlike unfolding in 6.6 nM VP15, unfolding in 33 nM VP15 was not stepwise. Consistently, the folding time course at the same VP15 concentration was not stepwise either (Fig. 3B). These observations suggest that at higher VP15 concentrations the DNA was folded into much tighter and more complex structures. Unfolding DNA condensed in even higher VP15 concentrations required even larger forces that exceeded the largest force our tweezer allowed (~30 pN).

VP15 folds DNA distinctly from multivalent cations and many other DNA folding proteins

We provided direct evidence that binding of VP15 to DNA led to DNA folding. The magnetic tweezer experiments showed that the DNA folding was able to withstand forces of a few pN when the VP15 concentrations were larger than 6.6 nM in PBS buffer. The AFM experiments further showed that the DNA molecules were folded by VP15 into various condensates in a VP15 concentration dependent manner. At 66 nM, the DNA was mainly folded into loops (Fig. 2A) and flower structures (Fig. 2B) and a significant portion of DNA remained unbound by VP15. At 660 nM, the mode of VP15 binding changed. Most of the DNA were bound by VP15, and the dominating condensates were bundles (Figs. 2C–F). At even higher concentrations (6.6 μM or above), striking nucleosome-like particles formed on the folded DNA. The VP15 induced DNA condensates are more complex than those formed by multivalent cations, where DNA is mainly condensed into regular toroid structures (Fu et al., 2006; Hud and Downing, 2001). They do not resemble the DNA organized by the abundant bacterial histone-like nucleoid structural protein (H-NS) either, where DNA are either folded into a perfect DNA hairpin structure in the presence of a few mM $MgCl_2$, or stiffened by homogeneous coat of a H-NS polymer on the DNA backbone at lower $MgCl_2$ concentration (Dame, 2005; Liu et al., 2010).

Comparison with previous research on VP15 — DNA interaction

EMSA assay of VP15 binding to the plasmid DNA (pET28a) was previously done by Witteveldt et al. (Witteveldt et al., 2005) . They showed that VP15 bound to circular and linearized plasmid DNA and could result in band disappearance when VP15 concentration exceeded certain threshold values. The band disappearance could be caused by DNA charge neutralization by VP15 or by formation of large DNA condensates. The authors proposed that it was due to the latter mechanism because they found that VP15 preferred binding to super-coiled plasmid. This mechanism is strongly supported by our AFM images which showed that the DNA were organized into VP15 concentration dependent DNA condensates. In addition, it was biochemically shown that VP15 can interact with itself to form homomultimers, but not with the other major structural proteins of WSSV (Witteveldt et al., 2005). The particle-like structures formed at 6.6 μM VP15 (Figs. 2G–H) suggests that regular VP15 homomultimers might form at 6.6 μM or higher concentrations and bind to DNA as nucleosome-like particles.

As shown in Figs. 2A–B, at 66 nM VP15, naked DNA and condensed DNA co-exist. Upon binding, VP15 tends to stay together, leaving the rest of the DNA naked (for example, as shown in Figs. 2A–B). Such a "phase separation" is a natural result of the cooperative binding of VP15 to DNA under unsaturated conditions where there are abundant DNA binding sites available for protein binding. Under unsaturated binding conditions, such cooperative binding of VP15 should eventually lead to two DNA species: one is naked DNA that does not contain VP15 (or nearly so), and the other is highly condensed DNA aggregates. In an EMSA experiment, the former will migrate at a speed same as (or nearly so) the native DNA, and the latter will be much slower or even not able to penetrate into the gel due to their large size and complex conformation. This prediction is in agreement with the EMSA assay using plasmid DNA (pET28a) (Witteveldt et al., 2005), and was confirmed in our experiments for linear Phix 174 DNA (Supplementary Fig. S2).

Implications on the function of VP15

As mentioned in the introduction, WSSV and baculoviruses share many characteristics (Bud and Kelly, 1980; Durand et al., 1998). It was evidenced that the baculovirus genome DNA is bound with a small, highly basic protein (Tweeten et al., 1980). Therefore, we hypothesize that the WSSV genome DNA is organized similarly. VP15 is one of the major capsid proteins identified and is highly basic; therefore, it is a promising candidate that organizes WSSV DNA in the capsid. This hypothesized role of VP15 is supported by the observation that he VP15 induced DNA condensates and the genome DNA leaked from fractured WSSV capsid (Figs. 1C–F) show a resemblance.

We are aware that such resemblance cannot be considered as direct evidence that the viral DNA in the WSSV virions are bound with abundant VP15. We have no knowledge of the physiological relevant concentration of VP15 during viral DNA packaging process in the host cells; therefore the concentrations of VP15 used in our studies were arbitrary and spanned over a large range from 66 nM to 6.6 μM. Our results, however, provide further insights to the understanding of the possible role of VP15. Overall our AFM imaging and single-DNA stretching experiments suggest that VP15 likely plays an important role in participating in the DNA packaging process by direct folding of the viral genome DNA.

Materials and methods

WSSV purification

WSSV was purified from hemolymph of artificially WSSV-infected red claw crayfish, Cherax quadricarinatus, by sucrose gradient centrifugation as previously described (Huang et al., 2001). Purified viruses suspended in TNE buffer (50 mM Tris, pH 7.4, 100 mM NaCl, 5 mM EDTA) were preserved in −80 °C for subsequent experiments.

Cloning, expression and purification of VP15

The WSSV gene encoding VP15 was cloned into a pGEX-6P-1 vector (N-terminal GST-tagged) and expressed in E. coli BL21 strain. GST-VP15 fusion proteins were first purified by affinity chromatography using a GST resin column (Glutathione Sepharose 4B, GE healthcare), followed by cleavage with PreScission™ Protease at 4 °C overnight to remove the GST-tag. VP15 was then bound to a SP Sepharose column (GE healthcare) and eluted with a buffer containing 2 mM DTT, 2 M NaCl, and 1 mM EDTA at pH 8.0. The purity of VP15 was examined by SDS-PAGE.

Magnetic-tweezer manipulation studies of DNA-VP15 interaction

48.5 kb λ-DNA molecules were end-labeled using biotin- and digoxygenin-labeled oligonucleotides (Smith et al., 1992). The biotin end of the DNA was then bound to a 2.8-μm-diameter paramagnetic bead (Dynalbeads M-280 Streptavidin, Invitrogen, Singapore), and the digoxygenin end was fixed to the edge of a thin $0^{\#}$ cover glass (Paul Marienfeld GmbH & Co.KG) coated with anti-digoxygenin (Roche Diagnostics, Singapore). The tweezer is able to stretch a single DNA in the focal plane of the objective (Yan et al., 2004), making it an ideal tool to study DNA structural transition dynamics (Fu et al., 2010), the organizations of large DNA in eukaryotic cells (Yan et al., 2007), and in bacterial cells (Liu et al., 2010; Skoko et al., 2005). Before addition of the protein, the force-extension curve of the dsDNA was measured and the persistence length was obtained by fitting the Marko–Siggia formula (Marko and Siggia, 1995) for forces from 0.5 pN up to 10 pN. The tether between the glass edge and the paramagnetic bead DNA was determined to be a single DNA if the value of the bending persistence is 44–53 nm. After force calibration, VP15 was diluted in PBS buffer and injected into the flow cell, and the extension of DNA under different forces was recorded in real time. All experiments were conducted at room temperature. A sketch of the tweezer is included in the supplementary materials (Fig. S3). More details of the magnetic tweezer can be found in the supplementary materials of our previous paper (Liu et al., 2010).

Atomic Force Microscopy imaging

WSSV suspended in PBS buffer were deposited onto freshly cleaved mica surface. After WSSV deposited onto the surface, distilled water was applied to remove the unbound viral particles. The samples were then dried by nitrogen gas flow and imaged by AFM in air. The complexes of VP15 and DNA were formed by incubating 10 ng of Phix174 DNA or 10 ng λ-DNA with different concentrations of VP15 in 200 μL PBS solution for 20 min at room temperature. The DNA concentration expressed as Molar concentration of DNA base pairs for

Fig. 2. AFM images of DNA-VP15 complexes obtained in tapping mode in air. (A–B) DNA-VP15 complexes after incubation of 5386 bp long Phix174 linear dsDNA with 66 nM VP15. VP15 synapse mediated large DNA loops (A), and flower-like DNA aggregates (B) were often observed. A significant fraction of DNA was unbound with VP15. (C–D) DNA-VP15 complexes after incubation of Phix 174 DNA with 660 nM VP15. The DNA were mostly folded into a bundle-like structures. No naked DNA was observed. (E–F) DNA-VP15 complexes after incubation of 48,502 bp λ-DNA with 660 nM VP15. The DNA structures resembled the ones formed on Phix 174 DNA at the same concentration (C–D), suggesting that the structures of VP15 mediated DNA condensates do not have a significant dependence on DNA size and sequence. (G–H) At VP15 concentrations of 6.6 μM or above, the condensation was dominated by forming nucleosome-like particles along DNA (these experiments were carried out using λ-DNA only). At each condition, more than 10 micrographs were imaged for the analysis. In the absence of DNA, at any concentrations, VP15 alone cannot form any structures that are comparable to these images in sizes and in conformations (Supplementary Fig. S4).

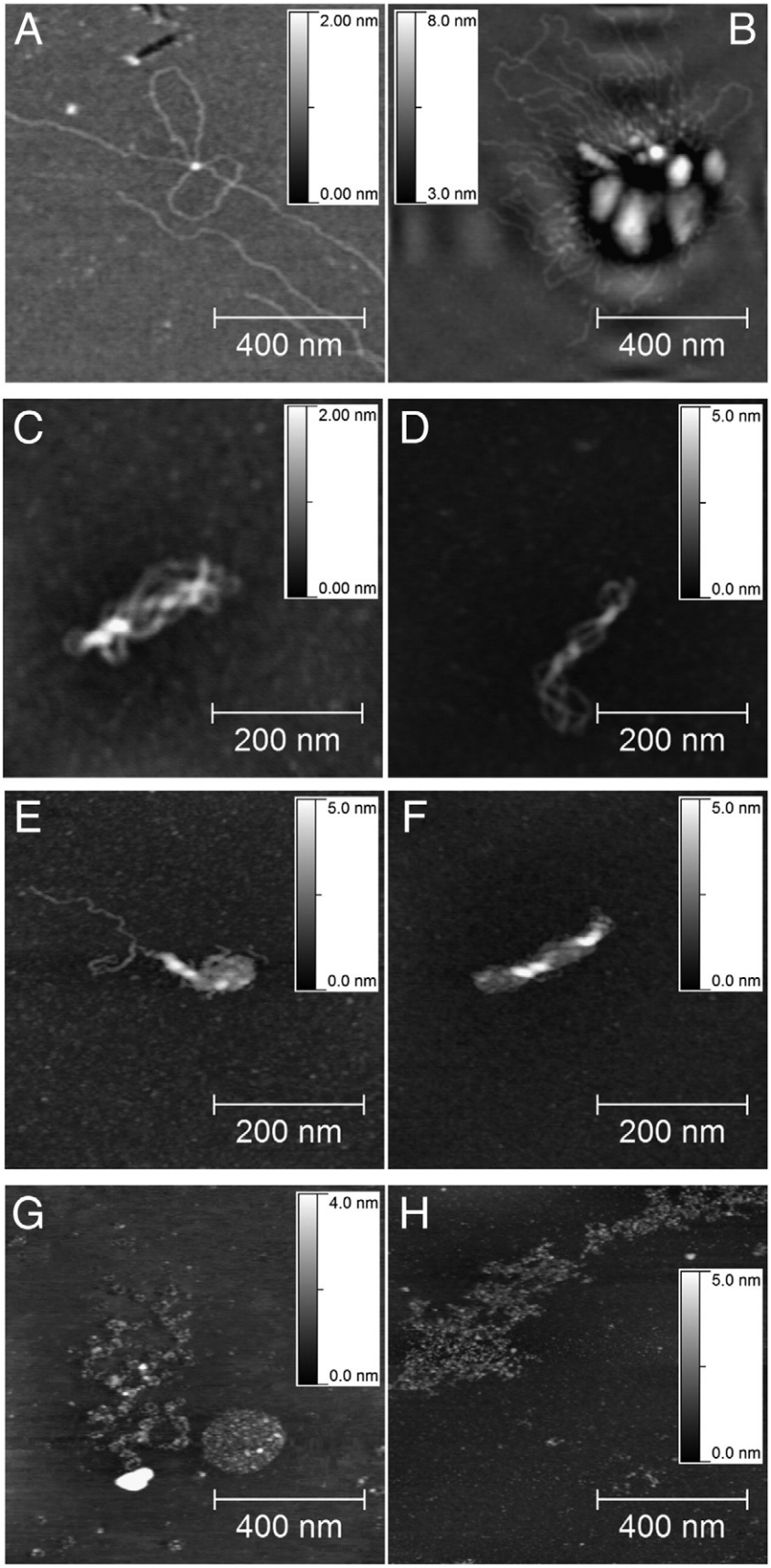
A
2.00 nm
0.00 nm
400 nm
B
8.0 nm
3.0 nm
400 nm
C
2.00 nm
0.00 nm
200 nm
D
5.0 nm
0.0 nm
200 nm
E
5.0 nm
0.0 nm
200 nm
F
5.0 nm
0.0 nm
200 nm
G
4.0 nm
0.0 nm
400 nm
H
5.0 nm
0.0 nm
400 nm

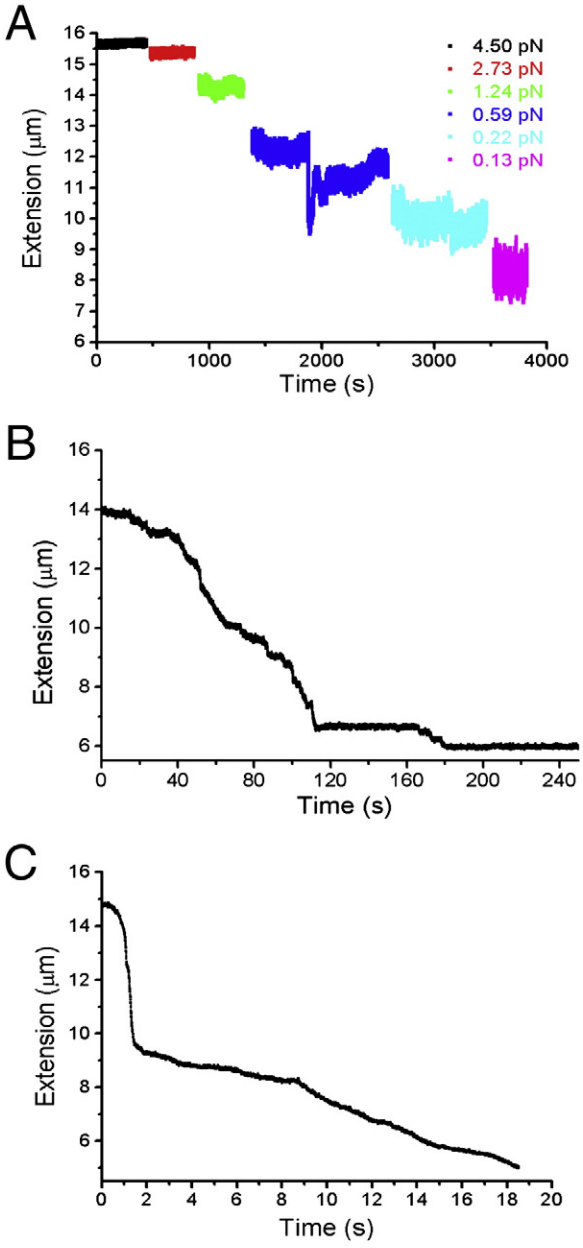

Fig. 3. DNA folding at different VP15 concentrations. (A) The dynamical change of the extension of a 48,502 bp long λ-DNA under different forces in the presence of 6.6 nM VP15 protein. Each force is denoted by a unique color, and its value is listed in the figure legend. Weak stepwise folding occurs at 1.24 pN, 0.59 pN, and 0.22 pN. Note: the stepwise decrease of extension occurs when force drops from a higher value to a lower one. It is not VP15 induced folding events, but elastic response of DNA. (B) Dramatic folding observed in the presence of 33 nM VP15 protein. The whole time course was recorded at a constant force of 2.76 pN. (C) In the presence of 66 nM, the folding was faster and could be against larger force. The time course was recorded at a constant force of 4.8 pN.

both types of DNA is around 76 nM, comparable to the concentrations of VP15 used in the experiments.

The mixture was then deposited onto glutaraldehyde-coated mica (Wang et al., 2005) for another 10 min at room temperature. These mica disks were then gently rinsed with distilled water, and dried by a steady stream of nitrogen. Images were acquired using Molecular Imaging 5500 AFM (Molecular Imaging, Agilent Technologies), operating in the tapping mode in air with silicon AFM probes (resonant frequency: 300 kHz, force constant: 40 N/m. Photoni Tech, Singapore).

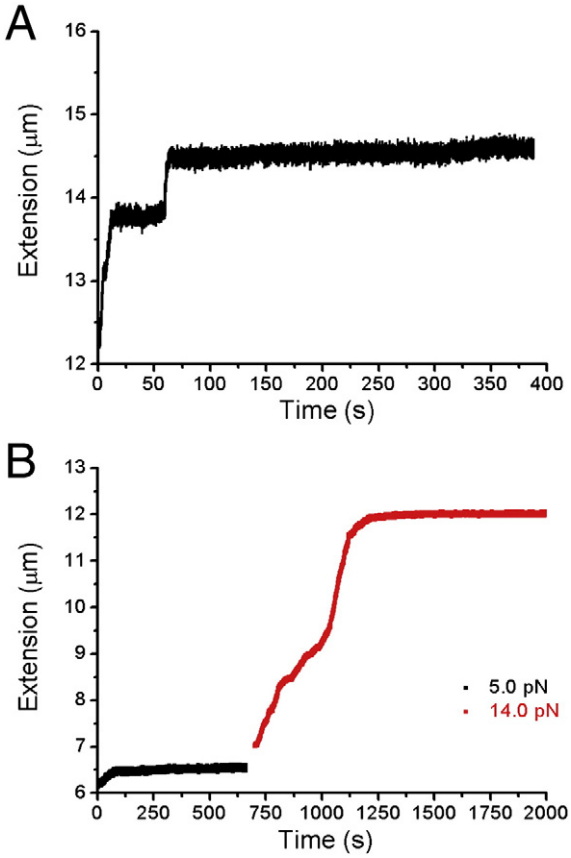

Fig. 4. DNA unfolding at larger forces. (A) The DNA folded in the presence of 6.6 nM VP15 could be unfolded at a constant force 3.1 pN. The unfolding time course displayed stepwise dynamics. (B) The DNA folded in 33 nM VP15 required much larger force to unfold. The DNA could not be unfolded at 5 pN (*black*) in about 10 min. Increasing the force to 14 pN (*red*) for more than 20 min, the DNA only unfolded to an extension about 12 μm. There was still about 4 μm DNA left unfolded. Apparently, the DNA was tightly folded in 33 nM VP15.

Acknowledgments

We thank Jack Johnson (Scripps Research Institute) for the helpful discussions. Individual efforts are as followed: experiments conducted by YL, JW, and HC; experiments conceived and paper written by CLH and JY. This work was supported by grants R144000192112 and R144000251112 from the Ministry of Education of Singapore (to JY), and grant R154000387112 from the Ministry of Education of Singapore (To CLH). We are also grateful for the financial support from the Mechanobiology Program at the National University of Singapore (now Mechanobiology Institute).

Appendix A. Supplementary data

Supplementary data to this article can be found online at doi:10.1016/j.virol.2010.09.008.

References

Borca, M.V., Irusta, P.M., Kutish, G.F., Carillo, C., Afonso, C.L., Burrage, A.T., Neilan, J.G., Rock, D.L., 1996. A structural DNA binding protein of African swine fever virus with similarity to bacterial histone-like proteins. Arch. Virol. 141 (2), 301–313.

Braunagel, S.C., Russell, W.K., Rosas-Acosta, G., Russell, D.H., Summers, M.D., 2003. Determination of the protein composition of the occlusion-derived virus of Autographa californica nucleopolyhedrovirus. Proc. Natl Acad. Sci. USA 100 (17), 9797–9802.

Bud, H.M., Kelly, D.C., 1980. An electron microscope study of partially lysed baculovirus nucleocapsids: the intranucleocapsid packaging of viral DNA. J. Ultra. Res. 73 (3), 361–368.

Dame, R.T., 2005. The role of nucleoid-associated proteins in the organization and compaction of bacterial chromatin. Mol. Microbiol. 56 (4), 858–870.
Deng, F., Wang, R., Fang, M., Jiang, Y., Xu, X., Wang, H., Chen, X., Arif, B.M., Guo, L., Hu, Z., 2007. Proteomics analysis of Helicoverpa armigera single nucleocapsid nucleopolyhedrovirus identified two new occlusion-derived virus-associated proteins, HA44 and HA100. J. Virol. 81 (17), 9377–9385.
Durand, S., Lightner, D.V., Bonami, J.R., 1998. Differentiation of BP-type baculovirus strains using in situ hybridization. Dis. Aquat. Org. 32 (3), 237–239.
Fu, H., Chen, H., Marko, J.F., Yan, J., 2010. Two distinct overstretched DNA states. Nucleic Acids Res. 38 (16), 5594–5600.
Fu, W.B., Wang, X.L., Zhang, X.H., Ran, S.Y., Yan, J., Li, M., 2006. Compaction dynamics of single DNA molecules under tension. J. Am. Chem. Soc. 128 (47), 15,040–15,041.
Huang, C., Zhang, L., Zhang, J., Xiao, L., Wu, Q., Chen, D., Li, J.K., 2001. Purification and characterization of White Spot syndrome virus (WSSV) produced in an alternate host: crayfish, Cambarus clarkii. Virus Res. 76 (2), 115–125.
Hud, N.V., Downing, K.H., 2001. Cryoelectron microscopy of lambda phage DNA condensates in vitreous ice: the fine structure of DNA toroids. Proc. Natl Acad. Sci. U. S. A. 98 (26), 14,925–14,930.
Hunt, M., 2010. Virology — Chapter Three. Microbiology and Immunology http://pathmicro.med.sc.edu/mhunt/dna1.htm (accessed 22 September 2010).
Ke, J., Wang, J., Deng, R., Wang, X., 2008. Autographa californica multiple nucleopolyhedrovirus ac66 is required for the efficient egress of nucleocapsids from the nucleus, general synthesis of preoccluded virions and occlusion body formation. Virology 374 (2), 421–431.
Krishnamoorthy, G., Roques, B., Darlix, J.L., Mely, Y., 2003. DNA condensation by the nucleocapsid protein of HIV-1: a mechanism ensuring DNA protection. Nucleic Acids Res. 31 (18), 5425–5432.
Lanier, L.M., Volkman, L.E., 1998. Actin binding and nucleation by Autographa california M nucleopolyhedrovirus. Virology 243 (1), 167–177.
Li, Z., Lin, Q., Chen, J., Wu, J.L., Lim, T.K., Loh, S.S., Tang, X., Hew, C.L., 2007. Shotgun identification of the structural proteome of shrimp white spot syndrome virus and iTRAQ differentiation of envelope and nucleocapsid subproteomes. Mol. Cell. Proteomics 6 (9), 1609–1620.
Liu, Y., Chen, H., Kenney, L.J., Yan, J., 2010. A divalent switch drives H-NS/DNA-binding conformations between stiffening and bridging modes. Genes Dev. 24 (4), 339–344.
Luijsterburg, M.S., White, M.F., van Driel, R., Dame, R.T., 2008. The major architects of chromatin: architectural proteins in bacteria, archaea and eukaryotes. Crit. Rev. Biochem. Mol. Biol. 43 (6), 393–418.
Marko, J.F., Siggia, E.D., 1995. Stretch DNAs. Macromolecules 28, 8759–8770.
Mayo, M.A., 2002. A summary of taxonomic changes recently approved by ICTV. Arch. Virol. 147 (8), 1655–1663.
Skoko, D., Yan, J., Johnson, R.C., Marko, J.F., 2005. Low-force DNA condensation and discontinuous high-force decondensation reveal a loop-stabilizing function of the protein Fis. Phys. Rev. Lett. 95 (20), 208–210.
Smith, S.B., Finzi, L., Bustamante, C., 1992. Direct mechanical measurements of the elasticity of single DNA molecules by using magnetic beads. Science 258 (5085), 1122–1126.
Sun, S., Kondabagil, K., Draper, B., Alam, T.I., Bowman, V.D., Zhang, Z., Hegde, S., Fokine, A., Rossmann, M.G., Rao, V.B., 2008. The structure of the phage T4 DNA packaging motor suggests a mechanism dependent on electrostatic forces. Cell 135 (7), 1251–1262.
Tweeten, K.A., Bulla, L.A., Consigli, R.A., 1980. Characterization of an extremely basic protein derived from granulosis virus nucleocapsids. J. Virol. 33 (2), 866–876.
van Hulten, M.C., Reijns, M., Vermeesch, A.M., Zandbergen, F., Vlak, J.M., 2002. Identification of VP19 and VP15 of white spot syndrome virus (WSSV) and glycosylation status of the WSSV major structural proteins. J. Gen. Virol. 83 (Pt 1), 257–265.
Wang, H., Bash, R., Lindsay, S.M., Lohr, D., 2005. Solution AFM studies of human Swi-Snf and its interactions with MMTV DNA and chromatin. Biophys. J. 89 (5), 3386–3398.
Wilson, M.E., Miller, L.K., 1986. Changes in the nucleoprotein complexes of a baculovirus DNA during infection. Virology 151 (2), 315–328.
Wilson, M.E., Mainprize, T.H., Friesen, P.D., Miller, L.K., 1987. Location, transcription, and sequence of a baculovirus gene encoding a small arginine-rich polypeptide. J. Virol. 61 (3), 661–666.
Witteveldt, J., Vermeesch, A.M., Langenhof, M., de Lang, A., Vlak, J.M., van Hulten, M.C., 2005. Nucleocapsid protein VP15 is the basic DNA binding protein of white spot syndrome virus of shrimp. Arch. Virol. 150 (6), 1121–1133.
Yan, J., Skoko, D., Marko, J.F., 2004. Near-field-magnetic-tweezer manipulation of single DNA molecules. Phys. Rev. E. Stat. Nonlin. Soft. Matter. Phys. 70 (1 Pt 1), 011905.
Yan, J., Maresca, T.J., Skoko, D., Adams, C.D., Xiao, B., Christensen, M.O., Heald, R., Marko, J.F., 2007. Micromanipulation studies of chromatin fibers in Xenopus egg extracts reveal ATP-dependent chromatin assembly dynamics. Mol. Biol. Cell 18 (2), 464–474.
Zhang, X., Xu, X., Hew, C.L., 2001. The structure and function of a gene encoding a basic peptide from prawn white spot syndrome virus. Virus Res. 79 (1–2), 137–144.